doi:10.1006/jmbi.2001.4966 available online at http://www.idealibrary.com on IDEAL® *J. Mol. Biol.* (2001) **312**, 823–832

JMB

The Structure of Helix III in *Xenopus* Oocyte 5 S rRNA: An RNA Stem Containing a Two-Nucleotide Bulge

Paul W. Huber[1]*, Jason P. Rife[2] and Peter B. Moore[3,4]

[1]*Department of Chemistry and Biochemistry, University of Notre Dame, Notre Dame IN 46556, USA*

[2]*Department of Medicinal Chemistry and the Institute for Structural Biology and Drug Discovery, Virginia Commonwealth University Richmond, VA 23298, USA*

[3]*Department of Chemistry*

[4]*Department of Molecular Biophysics and Biochemistry Yale University, New Haven CT 06520, USA*

**Corresponding author*

The solution structure of an oligonucleotide containing the helix III sequence from *Xenopus* oocyte 5 S rRNA has been determined by NMR spectroscopy. Helix III includes two unpaired adenosine residues, flanked on either side by G:C base-pairs, that are required for binding of ribosomal protein L5. The consensus conformation of helix III in the context provided by this oligonucleotide has the two adenosine residues located in the minor groove and stacked upon the 3′ flanking guanosine residue, consistent with biochemical studies of free 5 S rRNA in solution. A distinct break in stacking that occurs between the first adenosine residue of the bulge and the flanking 5′ guanosine residue exposes the base of the adenosine residue in the minor groove and the base of the guanosine residue in the major groove. The major groove of the helix is widened at the site of the unpaired nucleotides and the helix is substantially bent; nonetheless, the G:C base-pairs flanking the bulge are intact. The data indicate that there may be conformational heterogeneity centered in the bulge region. The corresponding adenosine residues in the *Haloarcula marismortui* 50 S ribosomal subunit form a dinucleotide platform, which is quite different from the motif seen in solution. Thus, the conformation of helix III probably changes when 5 S rRNA is incorporated into the ribosome.

Keywords: 5 S rRNA; ribosomal protein L5; bulged nucleotides; NMR spectroscopy

In eukaryotes, 5 S rRNA is transported from the nucleoplasm, where it is synthesized, to the nucleolus, where it is incorporated into ribosomes, bound to ribosomal protein L5. Thus, it appears that the L5-5 S rRNA complex is added to the ribosome as a discrete unit.[1] This ribonucleoprotein (RNP) particle can also be specifically removed from the large ribosomal subunit by a variety of methods.[2–4] In *Xenopus* oocytes, most of the 5 S rRNA synthesized during early oogenesis is stored in the cytoplasm bound either to transcription factor IIIA (TFIIIA) or to a homologous zinc finger protein, p43.[5–8] When ribosome synthesis begins during vitellogenesis, an exchange reaction occurs that results in the replacement of TFIIIA and p43 by L5, so that 5 S rRNA can be transported to the nucleolus.[9–11]

The binding site on 5 S rRNA for L5 overlaps those for TFIIIA and p43.[12,13] Nevertheless, the principal identity elements for L5 in *Xenopus* 5 S rRNA, which are located in the helix III-loop C hairpin, are not the same as those used by TFIIIA and p43, which are located in the helix II-loop A-helix V-loop E region of the molecule.[13-15] A two-adenosine bulge in helix III, which is conserved in 5 S rRNAs from all three kingdoms, appears to be particularly important for L5 binding. The affinity of L5 for 5 S rRNA falls by more than two orders of magnitude when these nucleotides are deleted.[14] As part of a continuing effort to understand the role of this conserved two-nucleotide bulge in L5 binding, we have determined the solution structure of a 22 nt RNA that contains the helix III sequence of *Xenopus* oocyte 5 S rRNA.

Abbreviations used: NOESY, nuclear Overhauser effect spectroscopy; HMQC, heteronuclear multiple quantum coherence; TOCSY, total correlation spectroscopy; COSY, correlated spectroscopy; DQF, double quantum filtered; rmsd, root-mean-square deviation; DEPC, diethylpyrocarbonate; RNP, ribonucleoprotein; TFIIIA, transcription factor IIIA.

E-mail address of the corresponding author: huber.1@nd.edu

0022-2836/01/040823–10 $35.00/0

Results

Helix III oligonucleotide

A 22 nt RNA oligonucleotide that should form a hairpin structure terminating with a GAGA tetraloop was prepared by *in vitro* transcription using phage T7 RNA polymerase. The sequence of its stem corresponds with helix III of *Xenopus* oocyte 5 S rRNA flanked on either side by a single G:C base-pair (Figure 1). There was no substantive difference between nuclear Overhauser effect (NOE) spectra of the 22-mer in the absence and in the presence of 4 mM magnesium, indicating that the conformation of this RNA does not depend on Mg^{2+} (data not shown). Interestingly, the binding of L5 to 5 S rRNA does not require Mg^{2+}, and binding affinity actually decreases at Mg^{2+} concentrations above 2 mM.[14] The chemical shift dispersion of the 22-mer was sufficiently good so that an isotopically labeled sample was not required for the assignment of proton resonances.

Assignments

The imino proton spectrum of the 22-mer is well resolved (Figure 2), and its resonances were readily assigned using nuclear Overhauser effect spectroscopy (NOESY) spectra collected in 90 % H_2O at 10 °C. Imino proton resonances were identified for all of the expected Watson-Crick base-pairs of the stem, including the terminal G:C pair. In addition, G9, which forms a sheared base-pair with A12 in the tetraloop, accounts for the most upfield imino resonance at 10.52 ppm.

Non-exchangeable proton resonance assignments were made using spectra acquired at 30 °C. The anomeric-aromatic region of a 300 ms ^2H_2O-NOESY spectrum (Figure 3) contains a sequential H1′ to H6/8 walk that can be traced from G1 to G9. Consistent with the spectra of other GNRA tetraloop structures,[16] a break in the walk occurs between G9 and A10. Stacking of the three bases on the 3′ side of the loop is supported by internucleotide NOEs between A10 and G11, and between G11 and A12. The position of A12 directly over the H1′ of C13 shifts its resonance substantially upfield. Despite the presence of a putative cross-peak corresponding to a backwards sequential between C13H1′ and A12H8, the chemical shift assignment of the former could not be confirmed in the natural abundance ^1H-^{13}C-HMQC spectrum and, therefore, is considered unassigned. The remainder of the walk from U14 to C22 is continuous, providing evidence for the intrahelical position of the two adenosine residues. The ^1H-^{13}C HMQC experiment was used to confirm the assignments of anomeric and aromatic proton resonances initially made from NOESY spectra. All aromatic resonances and, with the exception of C13, all H1′ and H2′ resonances were assigned from these spectra. In addition, several adenine H2 and pyrimidine H5 resonances were identified in homonuclear experiments.

A ^1H-^{31}P heteronuclear TOCSY-NOESY experiment was used to correlate H1′, H2′, aromatic and some H3′ resonances with those of 19 of the 21 phosphorus atoms in the molecule. The assignment of H3′ resonances in the hTOCSY-NOESY experiment were confirmed using data from ^1H-^{31}P hTOCSY and ^1H-^{31}P hCOSY experiments; three additional H3′ assignments were made in the latter experiment. A Table of chemical shifts of proton and phosphorus resonances is available as Supplementary Material.

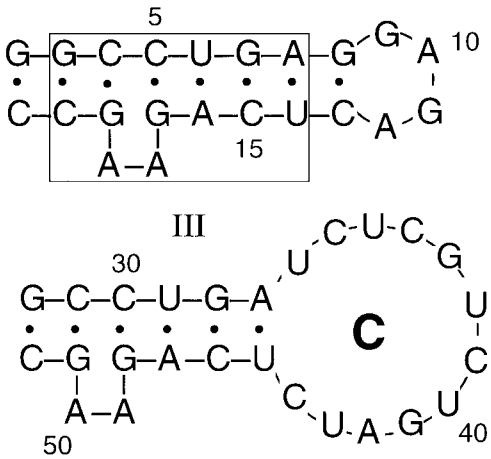

Figure 1. Sequence and secondary structure of the 22 nt RNA. The stem of the hairpin corresponds to helix III of *Xenopus* oocyte 5 S rRNA (boxed) flanked on each side by an additional G:C base-pair. The helix III-loop C hairpin from *Xenopus* oocyte 5 S rRNA is shown below for comparison.

Structural implications of spectral data

The imino proton resonances establish that the oligonucleotide forms the expected hairpin structure, including the terminal G1:C22 base-pair and the G9:A12 sheared base-pair in the tetraloop. The presence of assignable imino proton resonances for G17 and G20 in the exchangeable proton spectrum, as well as the existence of cross-peaks between those imino proton resonances and the amino protons of their cytosine partners in NOESY spectra, provide evidence that the C3:G20 and C4:G17 base-pairs flanking the bulge are normal Wastson-Crick base-pairs.

The unambiguous sequential NOE between C3H1′ and C4H6 indicates that the strand opposite the bulge has an A-type conformation, a conclusion reinforced by the sequential NOEs from the H2′ and H3′ protons of C3 to the H6 proton of C4 as well as between C3H6 and C4H6. Thus, the structure of this RNA must be distinctly different from that reported for an analogous DNA containing two bulged adenosines flanked by G:C base-pairs, where the absence of an anomeric to aromatic cross-peak between the two cytosine residues

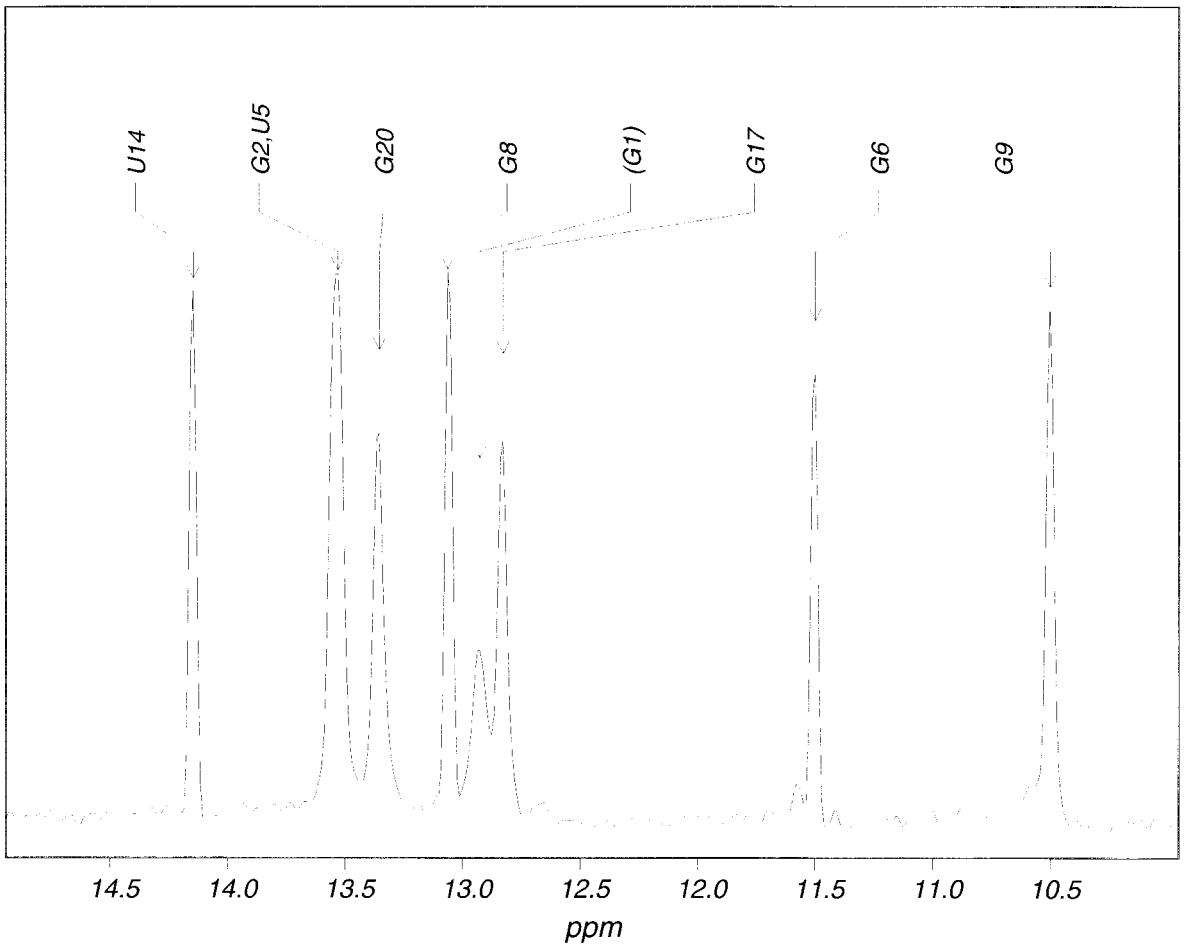

Figure 2. NMR spectrum of imino protons. The imino region of a one-dimensional spectrum collected at 10 °C is presented and accounts for all of the base-pairs expected for the hairpin structure of the 22-mer.

opposite the bulge indicated a backbone conformation that increases the distance between the two pyrimidine residues.[17]

The disposition of the unpaired adenosine residues and flanking guanosine residues across the bulge does not appear to be symmetrical, which is in agreement with predictions made from chemical probing experiments of RNA duplexes containing internal loops and bulges.[18] An A18H2 to A19H1′ cross-peak is not present in the NOESY spectrum; consequently, a distance constraint was included in the structure calculations to keep these protons more than 4.5 Å apart.[19] The H2 sequential cross-peak of the other adenosine residue in the bulge (A19H2 to G20H1′) is present, suggesting that the relative position of the two residues at the 3′ junction of the bulge is not greatly different from that of a base step in a canonical A-type helix. Otherwise, the H2 protons of the bulged adenine residues do not have identifiable NOEs to other aromatic resonances. In the same manner, putative aromatic-aromatic cross-peaks for A18 and A19, and for G17 and A18 are very weak, whereas, a cross-peak corresponding to A19H8 to G20H8 is clearly present.

NOESY spectra gave several indications that the bulge region of the molecule can exist in two different conformations. Cross-peaks involving anomeric resonances for G1, G2, C3, A16, G17, and G20 each exhibit a second, less intense resonance at both short and long mixing times, indicating an equilibrium on the hundreds of millisecond timescale or longer. We could find no evidence for aggregation or for length heterogeneity in the RNA sample that could account for the alternative set of resonances. The H1′ to C1′ cross-peak for G20 in a ^{1}H-^{13}C HMQC spectrum is a doublet, likewise indicating some structural heterogeneity in the bulge.

Based upon the observed weak to medium intensity of intranucleotide H1′ to H6/H8 NOEs, all nucleotides in the 22-mer appear to be in an *anti* conformation.

Information on ribose conformations came from measurements of H1′ to H2′ coupling constants in a DQF-COSY experiment.[20] The large scalar couplings for A18 and A19 (10-12 Hz) establish that the sugar conformation for the two nucleotides in the

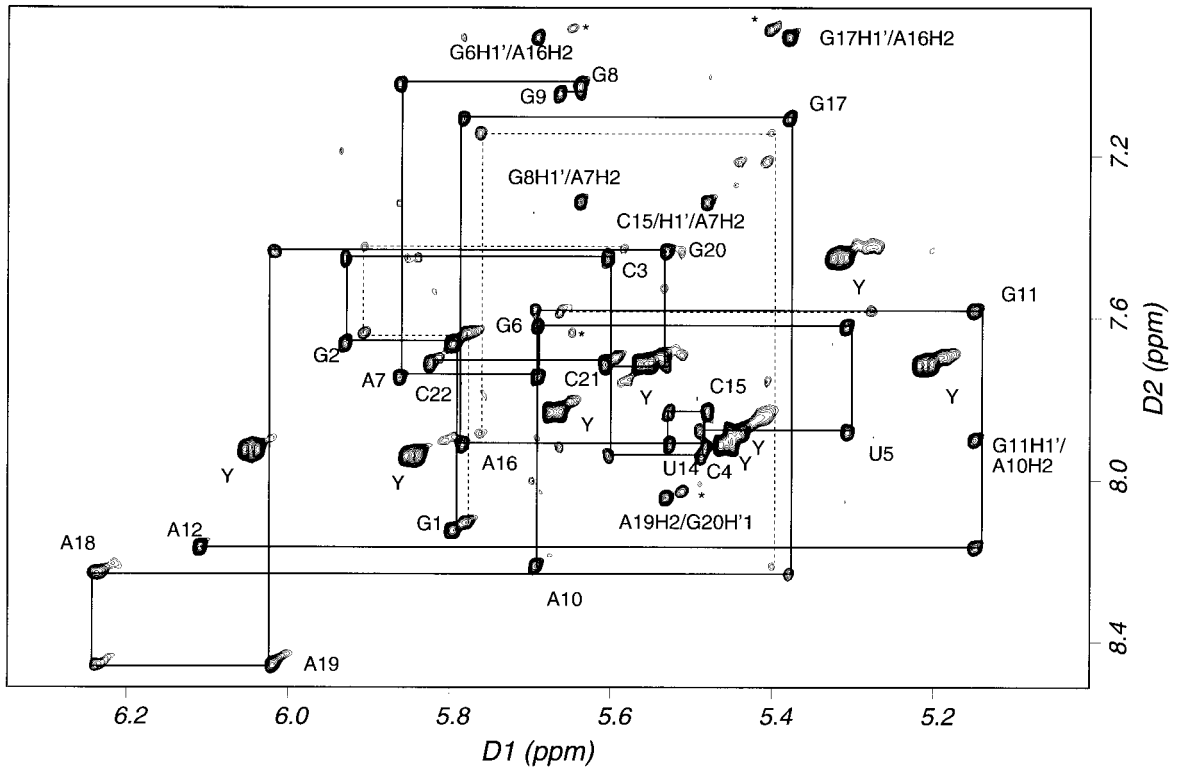

Figure 3. The anomeric-aromatic region of a 300 ms NOESY spectrum collected at 30 °C. A continuous line traces the anomeric to aromatic walk of the main cross-peaks, while a broken line traces the comparable connectivity of the secondary cross-peaks exhibited by nucleotides surrounding the bulge. The walk is broken at G9 and resumes at A12 within the tetraloop. Intranucleotide H1′ to H6/8 cross-peaks are designated by residue number, pyrimidine H5 to H6 cross-peaks by a "Y". Adenine H2 to H1′ cross-peaks are also indicated. Asterisks mark other secondary cross-peaks.

bulge is predominantly C2′ *endo*. Moderate coupling constants for A10, G11, A12, and G17 (5-6 Hz) indicate that the riboses at these positions are a mixture of C2′ *endo* and C3′ *endo* conformations. The 5′ and 3′ terminal nucleotides also exhibit large H1′ to H2′ coupling constants, presumably due to structural dynamics at the end of the helix. A strong NOE between the H2′ and H8 protons of A19 coupled with an extremely weak NOE between A18H2′ and A19H8 provided additional evidence for the C2′ *endo* conformation for the ribose of A19.

Structure of helix III

The 22 nt RNA used here has helix III of *Xenopus* oocyte 5 S rRNA capped with a GAGA tetraloop. Spectral features found in the NMR spectra confirm that the loop of this RNA adopts the expected GNRA tetraloop structure, which has been solved several times in other contexts by both NMR[21] and X-ray crystallography.[22] In order to increase the convergence rate in our structure calculations, we included artificial distance constraints that forced the four nucleotides of this loop to adopt a standard GNRA structure.

The set of NMR-derived restraints summarized in Table 1 were used to compute the structure of the 22-mer (see Materials and Methods). Of the 14 low energy, zero-violation structures that emerged, nine clearly fall into a single family in which the two adenosine residues of the bulge form a continuous stacked structure with G20 (Figure 4). In the five remaining structures, the position of A18 is quite variable, with the base of the residue generally unstacked and perpendicular to the flanking base-pairs (Figure 5). Thus, the data are consistent with at least two different arrangements of A18, and it is tempting to surmise that the observed doubling of bulge-related NOESY cross-peaks reflect that fact. However, it is important to note that the secondary set of NOEs mirrors the primary set; there are no unique NOEs identified in the former. Therefore, all 14 structures reported here are consistent with both the primary and secondary set of NOEs, which suggests that the data are insufficient to constrain the conformation of A18 any more precisely. When the bulge regions of all low energy structures are superimposed, the average pairwise root-mean-square deviation (rmsd) is 1.49 Å (Table 2). However, when A18 is excluded from the calculation, the rmsd decreases to 1.18 Å. A significant decrease in the rmsd also

Table 1. Experimental observations and resulting constraints used to solve the structure of helix III

Observation	Constraint	No.[a]
Nuclear Overhauser effect	Intraresidue distance	118
	Interresidue distance	115
	unoes	25
	Total	258
	NOEs per residue	11.7
	NOEs per residue (A18 and A19 only)	11
Anomeric-aromatic NOE	χ	22
H1′-H2′ coupling constant	ν_0-ν_4[b]	18
A-form stem	α	11
	β	12
	γ	12
	ε	12
	ζ	11
Exclusion of gauche$^+$ ε	ε	9
	Total dihedrals	178
	Total experimentals	436
	Constraints per residue	19.8
Watson-Crick base-pairs[c]	Distances defining base-pairs	44
Tetraloop sheared base-pair[c]	Distances defining base-pair	6

[a] Number of observations.
[b] Five angles are specified for each ribose, but they determine only one degree of freedom; therefore, each ribose is counted as only a single constraint.
[c] Not counted in constraints per residue calculation.

occurs when only the nine structures of the consensus family are compared (1.27 Å).

The structure of helix III presented in Figure 6 is the family member most similar to the average structure of the consensus family. The two adenosine residues of the bulge reside in the minor groove and form a continuous stack with G20. The C2′ *endo* conformation of these nucleotides enables the backbone to proceed from residue 20 to 18 with little helical twist, resulting in an increasing displacement of the three stacked bases into the minor groove. The helical discontinuity caused by the shift of the adenosine residues into the minor groove opens the major groove, which exposes one side of the base of G17 to solvent, consistent with results using an intercalative structural probe that indicated an enlarged major groove at the site of the bulge.[23]

Table 2. Structural statistics and atomic rmsd

	Mean value
rmsd of distance constraints (Å)	0.0137
rmsd of dihedral angle (deg.)[a]	0.113
rmsd from idealized geometry	
Bonds (Å)	0.0014
Angles (deg.)	2.20
Heavy-atom rmsd (Å)[b]	
All RNA	1.60
Bulge (residues 3-5 & 16-20)	1.49
Bulge (without residue 18)	1.18
Bulge of consensus family	1.27

[a] Refers to experimental dihedral values not force-field defined dihedral terms.
[b] The average of the pairwise rmsd values to the average structure.

A distinct break occurs between A18 and G17 with the bases of these two residues unstacked and oriented at an approximate 45° angle. This upward tilt of A18 combined with some propeller twisting in the C4:G17 base-pair puts the H61 proton of A18 within hydrogen bond distance of C4O2 (N—O distance of 2.7 Å). This interaction may help stabilize the predominant conformation of A18, since it is lost in all of the other structures in which the base is unstacked and perpendicular to the adjacent base-pairs. A similar type of interaction has been reported in the structure of a helix containing an unpaired adenosine residue with an A:U base-pair in the 5′ flanking position.[24] In this latter case, the bulged adenosine residue is protonated at N1 and forms an interstrand hydrogen bond to the O2 position of the uridine residue in the adjacent base-pair that exhibits an even greater propeller twist (~30°) than the C4:G17 base-pair in helix III. Significantly, the bulged adenosine residue in this structure is also partially displaced towards the minor groove.

The unstacking of A18 and G17 exposes the bases of both residues to solvent and this disruption is apparent in the NOE interactions between these two nucleotides. Although a sequential anomeric-aromatic cross-peak between G17 and A18 is apparent at most mixing times, its intensity is diminished somewhat relative to the other peaks in the connectivity pattern. In addition, the aromatic-aromatic NOEs between A18 and its neighbors, G17 and A19, are weaker than the corresponding NOEs between A19 and G20, and A16 and G17. The H2′ and H3′ protons of G17, however, exhibit strong NOE interactions with the H8 proton of A18.

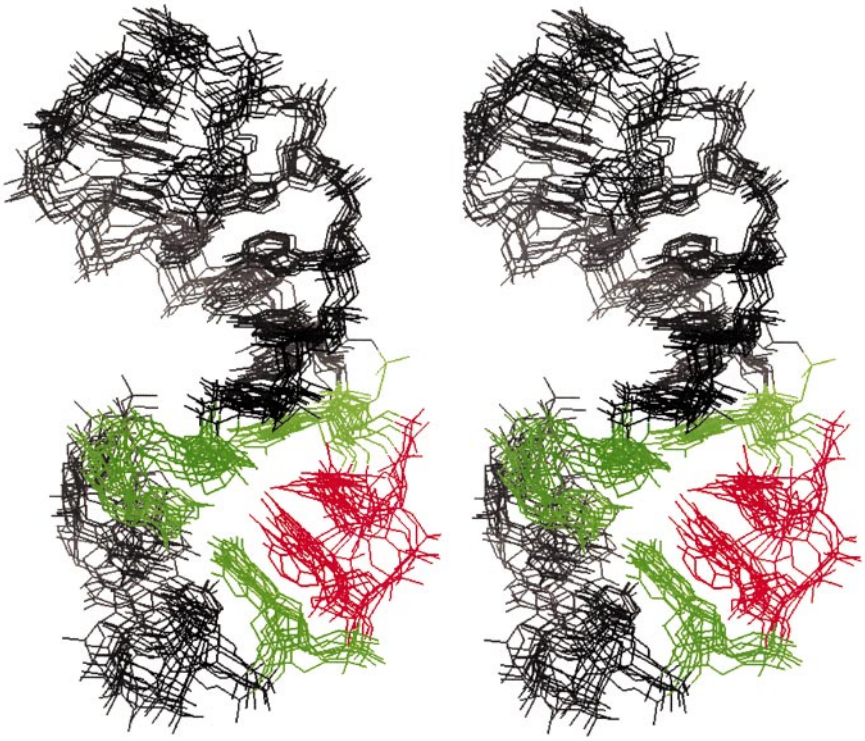

Figure 4. Superposition of the nine structures that define the consensus conformation onto the average structure. The molecules were superimposed using the heavy atoms of all nucleotides. The average pairwise rmsd between each structure and the average structure is 1.409 Å. The unpaired adenosines of the bulge (18 and 19) are red; the G:C base-pairs flanking the bulge are green.

It is well known that unpaired bases are associated with kinks and/or bends in RNA and DNA helices.[25] It is not surprising, then, that A18 and A19 cause a pronounced bend in helix III that increases the exposure of the base of A18 to solvent (Figure 6). The bend appears to compensate, at least in part, for the differences in the twist of the two strands at the site of the bulge, but the data are not sufficient to define its magnitude. The helices flanking the bulge fit a consensus A-type conformation with no significant distortion of the base-pairs adjacent to the unpaired nucleotides other than a moderate increase in propeller twisting.

Discussion

The structure described above shows that two unpaired adenosine residues can assume an intrahelical position in the minor groove of an RNA stem without disruption of the flanking base-pairs and with no obvious distortion of the base steps opposite the bulge. It is equally clear, however, that this structure is not the only possible conformation for bulges of this kind or the only conformation consistent with our data. Evidence for structural heterogeneity, centered at the bulge, is apparent in the anomeric-aromatic region of the $^{2}H_{2}O$-NOESY spectrum, but can also be seen in other regions, such as that which includes the H1′ to H2′ cross-peaks.

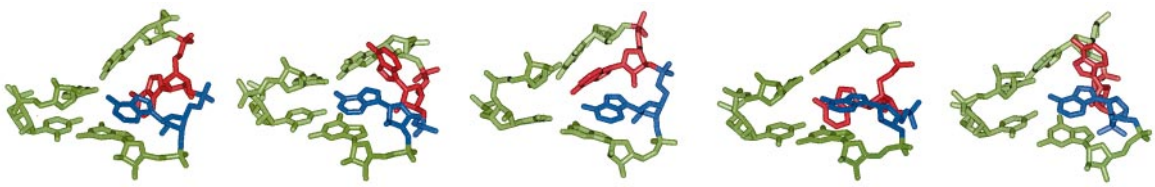

Figure 5. Alternative conformations of the bulge. The bulge region of the five alternative, low-energy, zero-violation structures demonstrate the different conformations that A18 (red) may sample. The remainder of the molecule remains essentially unchanged in these structures. A19 is blue and the G:C base-pairs flanking the bulge are green.

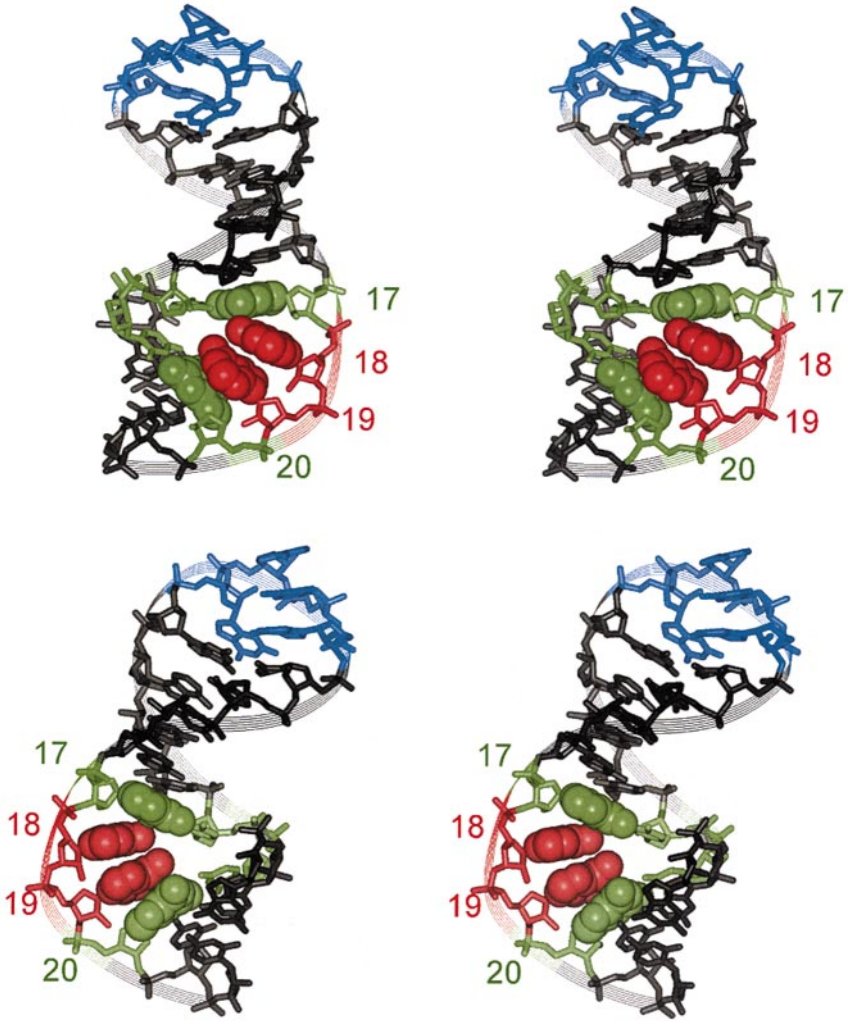

Figure 6. Stereo views of the structure of the hairpin. Nucleotides 9-12, which comprise the tetraloop are blue; the unpaired adenosine residues of the bulge (18 and 19) are red; the base-pairs flanking the bulge are green. The bulged adenosine residues and flanking guanosine residues are presented in CPK format to highlight the exposure of the base of A18 in the minor groove (top) and G17 in the major groove (bottom).

The structure of a DNA duplex having a two-nucleotide adenosine bulge, also flanked by guanosine residues, has been studied by NMR spectroscopy.[17] Both unpaired adenosine residues are inserted into the DNA helix with the flanking (G:C) base-pairs intact, but unlike the RNA structure, the adenosine residues reside in the major groove of the DNA helix. Furthermore, the conformation of the DNA backbone on the strand opposite the bulge is altered, so that the overall separation of the contiguous cytosine residues increases. There is no evidence for this type of deformation in the RNA helix examined here. A unique conformation for the two-nucleotide bulge in the DNA helix was not determined; however, by comparison with other NMR data, the authors suggested that continuous stacking occurs across the unpaired and flanking nucleotides.[17]

Continuous base stacking across the RNA bulge does not occur in any of the low energy, zero-violation structures we obtained. The consequence is that bases at the site of the bulge are exposed and this accessibility is further enhanced by the bend in the helical axis. The discontinuity in stacking across the bulge in helix III is in accord with thermodynamic evidence that asymmetric loops disrupt stacking between the flanking helices in RNA.[18] Moreover, major groove accessibility, measured by acylation of the N7 position of purine residues, was shown to be markedly increased for bulges of two or more nucleotides.[18]

While the work above was in progress, the structure of the 50 S ribosomal subunit from *Haloarcula marismortui* was solved at 2.4 Å resolution.[26] The conformation of the two-adenosine bulge in helix III of *H. marismortui* 5 S rRNA is entirely different from the one reported here. Rather than being inserted into the helix as a stacked pair, the two adenosine residues in question form an A-platform similar to the ones first identified in the P4-P6 domain of the *Tetrahymena* group I self-splicing intron.[27] In an A-

platform, two adenosine residues adjacent in sequence are oriented so that their bases are approximately coplanar and the N6 of the 3′ base is close to the N3 of its 5′ neighbor.

It is clear from earlier chemical probing data and the present NMR data that, outside the context provided by the ribosome, the unpaired adenosines in helix III do not form an A-platform either in intact 5 S rRNA or in the oligonucleotide studied here. The N7 position of both bulged adenosines is accessible to alkylation in *Xenopus*[28,29] as well as *Escherichia coli*[30] 5 S rRNA. In *Xenopus* oocyte 5 S rRNA, the N7 position of the residue corresponding to A19 is more susceptible to carbethoxylation than A18.[28] The reason for this difference in reactivity is apparent in the structure determined here. The N7 of A18 is found at the bottom of a particularly deep major groove, and access to it is blocked partially by the unstacking that places G17 in the major groove. Access to the N7 of A19 is unobstructed. Conversely, the co-planar platform arrangement of the adenosine residues in the *H. marismortui* 50 S subunit precludes alkylation of the N7 position of the residue corresponding to A19.

The bulged adenosines in helix III of *Xenopus* 5 S rRNA also react with dimethyl sulfate at their N1 positions.[28,29] In accord with this data, both of these nitrogen atoms are accessible in the minor groove of the average structure. The N1 position of the 5′ adenosine in a platform structure is usually unreactive;[27] however, examination of the *H. marismortui* structure reveals that the N1 position of both adenosine residues particularly the 3′ residue, are buried in the helix and poorly accessible to solvent.

Evidence from NOE experiments also supports the stacked conformation of the unpaired adenosine residues as opposed to the platform structure. This includes a weak NOE between A18H8 and A19H8, which are nearly 7 Å apart in the *H. marismortui* structure, and the absence of a cross-peak corresponding to A18H2 and C4H1′, which are within 3.9 Å in the 50 S subunit.

Together, these results substantiate the view that the NMR structure represents the conformation of helix III in free 5 S rRNA and that this region of the molecule undergoes a structural transition upon incorporation into the ribosome. Indeed, prokaryotic (*E. coli* L18) and eukaryotic (*Xenopus* L5) homologues of the archaeal protein (L18) that binds to the helix III region induce conformational changes in 5 S rRNA. Both proteins increase the positive ellipticity centered at 270 nm in the circular dichroism spectrum of the RNA, revealing a protein-dependent increase in base stacking (J. P. DiNitto & P.W.H., unpublished results).[30–32] To date, all platform structures appear to be stabilized either by base stacking interactions[27,33] or formation of base-triples.[34–37] In the *H. marismortui* structure there are no interactions of these sorts that can account for the side-by-side arrangement of the adenosines. Thus, this may be the first example where formation of an A-platform is dependent on protein binding rather than RNA tertiary interactions.

Materials and Methods

Sample preparation

The RNA oligonucleotide was synthesized by run-off transcription using T7 RNA polymerase. The product was purified by electrophoresis on 20 % polyacrylamide gels containing 7 M urea and recovered from gel slices by electroelution. Samples were dialyzed against buffer containing 5 mM sodium cacodylate (pH 6.5), 100 mM KCl, and then the volume reduced using a Centricon-3 (Amicon) filter unit. The sample in H_2O contained 10 % ^2H_2O and 0.006 % dioxane (chemical shift standard) and the final RNA concentration was 2.2 mM. A sample of the 22-mer in ^2H_2O was prepared by lyophilization (three times from 99.9 % ^2H_2O and once from 99.996 % ^2H_2O) and dissolved in 99.996 % ^2H_2O (Cambridge, Inc.) to a final concentration of 2.1 mM.

NMR spectroscopy

Proton and heteronuclear NMR spectra were collected on a GE Omega 500 MHz, Varian Unity 500 MHz, Varian Unity Plus 600 MHz, or Varian Inova 800 MHz spectrometers. Protons were referenced to the internal dioxane peak at 3.741 ppm. Phosphorus chemical shifts were references to an external trimethylphosphate standard (0.00 ppm). Spectra in H_2O were collected using a water-gate-water-flipback pulse sequence to suppress the large water signal.[38] Spectral data was processed using Felix 95.0 (MSI/Biosym, Inc.).

Structure calculations

Distance constraints assigned for non-exchangeable protons were based upon cross-peak intensities in 2D NOESY spectra collected at mixing times of 50, 150 or 300 ms. NOEs were classified as strong (distance range of 1.6-3.0 Å), medium (2.0-4.2 Å), weak (3.0-5.5 Å), or undetermined (1.6-5.5 Å). The structure was computed using 22 non-experimental constraints to ensure that the terminal tetraloop would always emerge in a standard GNRA conformation, which is consistent with the data qualitatively, and the 436 experimental constraints described in Table 1. A total of 25 of the experimental distance constraints used, which we identify as ''unoes'', were included to keep all loop aromatic and anomeric protons that did not give NOEs more than 4.5 Å apart. The unoes were included only for those aromatic-aromatic and aromatic-anomeric juxtapositions that would have produced NOEs in otherwise empty regions of helix III's NOESY spectra. Traditionally, our group, as well as others, have used unoes to exclude calculated structures not supported by NOESY data.[21,39–41] Here and in previous work, unoes were included en masse, from the outset of structure computations, without knowledge of which structures their presence prevents.

Dihedral angles were kept within 30° of standard A-conformation values for residues 1, 2, 5, 6, 7, 14, 15, 21, and 22. The torsion angles ε and ζ of residues 3, 8, and 16 , and α, β, and γ of residues 4, 13, and 20 were not restrained. Because there is no information for residues in the loop and bulge, only values for χ were restrained for residues 9-12 and 17-19.

A family of structures was generated using torsion angle molecular dynamics (TAMD) followed by simulated annealing in Cartesian space.[19,42,43] This family of structures was pruned to a subset in which the individual members contained no violations of experimentally derived distance or dihedral restraints and clustered to a similar lowest energy range (−207.3 to −245.7 energy units).

Accession number

The coordinates of the nine lowest energy structures are being deposited into the RCSB Protein Data Bank at Brookhaven, with accession code 1JUR.

Acknowledgments

This work was supported by grants from the National Institutes of Health to P.W.H. (GM38200) and P.B.M. (GM61258). We are grateful to Professor C. S. Chow (Wayne State University) for synthesis of oligoribonucleotides used in preliminary experiments, to Dr J. L. Diener for help with the ^{1}H-^{31}P HCOSY experiment, and to the members of the Moore Laboratory for their help and hospitality during P.W.H.'s stay.

References

1. Steitz, J. A., Berg, C., Hendrick, J. P., La Branche-Chabot, H., Metspalu, A., Rinke, J. & Yario, T. (1988). A 5 S rRNA/L5 complex is a precursor to ribosome assembly in mammalian cells. *J. Cell Biol.* **106**, 545-556.
2. Blobel, G. (1971). Isolation of a 5 S RNA-protein complex from mammalian ribosomes. *Proc. Natl Acad. Sci. USA,* **68**, 1881-1885.
3. Isoda, N., Tanaka, T. & Ishikawa, K. (1981). Isolation of a 5 S RNA-protein L5 complex from 60 S subunits of rat liver ribosomes by cesium sulfate density-gradient equilibrium centrifugation. *J. Biochem.* **90**, 551-554.
4. Marion, M. J. & Reboud, J. P. (1981). An argument for the existence of a natural complex between protein L5 and 5 S RNA in rat liver 60-S ribosomal subunits. *Biochim. Biophys. Acta,* **652**, 193-203.
5. Picard, B. & Wegnez, M. (1979). Isolation of a 7 S particle from *Xenopus laevis* oocytes: a 5 S RNA-protein complex. *Proc. Natl Acad. Sci. USA,* **76**, 241-245.
6. Pelham, H. R. B. & Brown, D. D. (1980). A specific transcription factor that can bind either the 5 S RNA gene or 5 S RNA. *Proc. Natl Acad. Sci. USA,* **77**, 4170-4174.
7. Honda, B. M. & Roeder, R. G. (1980). Association of a 5 S gene transcription factor with 5 S RNA and altered levels of the factor during cell differentiation. *Cell,* **22**, 119-126.
8. Joho, K. E., Darby, M. K., Crowford, E. T. & Brown, D. D. (1990). A finger protein structurally similar to TFIIIA that binds exclusively to 5 S RNA in *Xenopus*. *Cell,* **61**, 293-300.
9. Rudt, F. & Pieler, T. (1996). Cytoplasmic retention and nuclear import of 5 S ribosomal RNA containing RNPs. *EMBO J.* **15**, 1383-1391.
10. Murdoch, K. J. & Allison, L. A. (1996). A role for ribosomal protein L5 in the nuclear import of 5 S rRNA in *Xenopus* oocytes. *Exp. Cell Res.* **227**, 332-343.
11. North, M. T. & Allison, L. A. (1998). Nucleolar targeting of 5 S RNA in *Xenopus laevis* oocytes: somatic-type nucleotide substitutions enhance nucleolar localization. *J. Cell. Biochem.* **69**, 490-505.
12. Huber, P. W. & Wool, I. G. (1986). Use of the cytotoxic nuclease α-sarcin to identify the binding site on eukaryotic 5 S ribosomal ribonucleic acid for the ribosomal protein L5. *J. Biol. Chem.* **261**, 3002-3005.
13. Zang, W.-Q. & Romaniuk, P. J. (1995). Characterization of the 5 S RNA binding activity of *Xenopus* zinc finger protein p43. *J. Mol. Biol.* **245**, 549-558.
14. Scripture, J. B. & Huber, P. W. (1995). Analysis of the binding of *Xenopus* ribosomal protein L5 to oocyte 5 S rRNA: the major determinants of recognition are located in helix III-loop C. *J. Biol. Chem.* **270**, 27358-27365.
15. Rawlings, S. L., Matt, G. D. & Huber, P. W. (1996). Analysis of the binding of *Xenopus* transcription factor IIIA to oocyte 5 S rRNA and to the 5 S rRNA gene. *J. Biol. Chem.* **271**, 869-877.
16. Heus, H. A. & Pardi, A. (1991). Structural features that give rise to the unusual stability of RNA hairpins containing GNRA loops. *Science,* **253**, 191-194.
17. Rosen, M. A., Live, D. & Patel, D. J. (1992). Comparative NMR study of A(n)-bulge loops in DNA duplexes: intrahelical stacking of A, A-A, and A-A-A bulge loops. *Biochemistry,* **31**, 4004-4014.
18. Weeks, K. M. & Crothers, D. M. (1993). Major groove accessibility of RNA. *Science,* **261**, 1574-1577.
19. Rife, J. P., Stallings, S. C., Correll, C. C., Dallas, A., Steitz, T. A. & Moore, P. B. (1999). Comparison of the crystal and solution structures of two RNA oligonucleotides. *Biophys. J.* **76**, 65-75.
20. Kim, Y. & Prestegard, J. H. (1989). Measurements of vicinal couplings from cross peaks in COSY spectra. *J. Magn. Reson.* **84**, 9-13.
21. Jucker, F. M., Heus, H. A., Yip, P. F., Moors, E. H. & Pardi, A. (1996). A network of heterogeneous hydrogen bonds in GNRA tetraloops. *J. Mol. Biol.* **264**, 968-980.
22. Correll, C. C., Wool, I. G. & Munishkin, A. (1999). The two faces of the *Escherichia coli* 23 S rRNA sarcin/ricin domain: the structure at 1.11 Å resolution. *J. Mol. Biol.* **292**, 275-287.
23. Chow, C. S., Hartmann, K. M., Rawlings, S. L., Huber, P. W. & Barton, J. K. (1992). Delineation of structural domains in eukaryotic 5 S rRNA with a rhodium probe. *Biochemistry,* **31**, 3534-3542.
24. Smith, J. S. & Nikonowicz, E. P. (1998). NMR structure and dynamics of an RNA motif common to the spliceosome branch-point helix and the RNA-binding site for phage GA coat protein. *Biochemistry,* **37**, 13486-13498.
25. Lilley, D. M. J. (1995). Kinking of DNA and RNA by base bulges. *Proc. Natl Acad. Sci. USA,* **92**, 7140-7142.
26. Ban, N., Nissen, P., Hansen, J., Moore, P. B. & Steitz, T. A. (2000). The complete atomic structure of the large ribosomal subunit at 2.4 Å resolution. *Science,* **289**, 905-920.
27. Cate, J. H., Gooding, A. R., Podell, E., Zhou, K., Golden, B. L., Szewczak, A. A., Kundrot, C. E., Cech, T. R. & Doudna, J. A. (1996). RNA tertiary structure mediation by adenosine platforms. *Science,* **273**, 1696-1699.
28. Christiansen, J., Brown, R. S., Sproat, B. S. & Garrett, R. A. (1987). *Xenopus* transcription factor IIIA binds primarily at junctions between double

helical stems and internal loops in oocyte 5 S RNA. *EMBO J.* **6**, 453-460.
29. Romaniuk, P. J., Leal de Stevenson, I., Ehresmann, C., Romby, P. & Ehresmann, B. (1988). A comparison of the solution structures and conformational properties of the somatic and oocyte 5 S rRNAs of *Xenopus laevis*. *Nucl. Acids Res.* **16**, 2295-2312.
30. Christensen, A., Mathiesen, M., Peattie, D. & Garrett, R. A. (1985). Alternative conformers of 5 S ribosomal RNA and their biological relevance. *Biochemistry,* **24**, 2284-2291.
31. Bear, D. G., Schleich, T., Noller, H. F. & Garrett, R. A. (1977). Alteration of 5 S RNA conformation by ribosomal proteins L18 and L25. *Nucl. Acids Res.* **4**, 2511-2526.
32. Spierer, P., Bogdanov, A. A. & Zimmermann, R. A. (1978). Parameters for the interaction of ribosomal proteins L5, L18, and L25 with 5 S RNA from *Escherichia coli*. *Biochemistry,* **17**, 5394-5398.
33. Butcher, S. E., Dieckmann, T. & Feigon, J. (1997). Solution structure of a GAAA tetraloop receptor RNA. *EMBO J.* **16**, 7490-7499.
34. Zimmermann, G. R., Jenison, R. D., Wick, C. L., Simorre, J. P. & Pardi, A. (1997). Interlocking structural motifs mediate molecular discrimination by a theophylline-binding RNA. *Nature Struct. Biol.* **4**, 644-649.
35. Amarasinghe, G. K., De Guzman, R. N., Turner, R. B. & Summers, M. F. (2000). NMR structure of stem-loop SL2 of the HIV-1 Ψ RNA packaging signal reveals a novel A-U-A base-triple platform. *J. Mol. Biol.* **299**, 145-156.
36. Conn, G. L., Draper, D. E., Lattman, E. E. & Gittis, A. G. (1999). Crystal structure of a conserved ribosomal protein-RNA complex. *Science,* **284**, 1171-1174.
37. Wimberly, B. T., Guymon, R., McCutcheon, J. P., White, S. W. & Ramakrishnan, V. (1999). A detailed view of a ribosomal active site: the structure of the L11-RNA complex. *Cell,* **97**, 491-502.
38. Lippens, G., Dhalluin, C. & Wieruszeski, J.-M. (1995). Use of a water flip-back pulse in the homonuclear NOESY experiment. *J. Biomol. NMR,* **5**, 327-331.
39. Dallas, A. & Moore, P. B. (1997). The loop E-loop D region of *Escherichia coli*: 5 S rRNA: the solution structure reveals an unusual loop that may be important for binding ribosomal proteins. *Structure,* **5**, 1639-1653.
40. Chang, K. Y. & Tinoco, I., Jr. (1997). The structure of an RNA "kissing" hairpin complex of the HIV TAR hairpin loop and its complement. *J. Mol. Biol.* **269**, 52-66.
41. Rife, J. P. & Moore, P. B. (1998). The structure of a methylated tetraloop in 16 S ribosomal RNA. *Structure,* **6**, 747-756.
42. Stallings, S. C. & Moore, P. B. (1997). The structure of an essential splicing element: stem loop IIa from yeast U2 snRNA. *Structure,* **5**, 1173-1185.
43. Stein, E. G., Rice, L. M. & Brünger, A. T. (1997). Torsion-angle molecular dynamics as a new efficient tool for NMR structure calculation. *J. Magn. Reson.* **124**, 154-164.

Edited by I. Tinoco

(Received 29 May 2001; received in revised form 18 July 2001; accepted 23 July 2001)

http://www.academicpress.com/jmb

A Table of chemical shift assignments is available as supplementary material on IDEAL